Journal of Materials Science: Materials in Electronics (2020) 31:2575–2582
https://doi.org/10.1007/s10854-019-02796-7

Towards an ink-based method for the deposition of $Zn_xCd_{1-x}S$ buffer layers in CZTS solar cells

Mirko Congiu[1] · Matteo Bonomo[2] · Diego di Girolamo[1] · Carlos F. O. Graeff[3] · Claudia Malerba[4] · Matteo Valentini[4] · Alberto Mittiga[4] · Danilo Dini[1]

Received: 11 November 2019 / Accepted: 20 December 2019 / Published online: 2 January 2020

Abstract

This work explores two different deposition methods to grow buffer layers of $Zn_xCd_{1-x}S$ for application in kesterite (Cu_2ZnSnS_4 (CZTS)) solar cells. The introduction of the mixed sulfide of Cd and Zn in CZTS based solar cells represents an important progress due to the improved device performance and minor toxicity with respect to sole CdS. The explored techniques are the chemical bath deposition (CBD) and the precursor ink. For the CBD we focused on the inclusion of zinc into the buffer, i.e. the target solid solution, taking into account the difference in the solubilities of ZnS and CdS. In aqueous solutions the co-deposition process is controlled by various solubility equilibria with CdS precipitation representing the most favorable process. Under these circumstances the ink method here proposed is a promising approach since it is based on the thermal degradation of stable chemical precursors deposited on a dry film. In doing so, the problematic co-deposition of a mixed sulfide derived from sulfides with considerably different solubilities is circumvented. The most important advantages of this approach are the easiness and scalability of the whole process and the reduction of the amounts of toxic reagents/products.

1 Introduction

The main challenge in the development of Cu_2ZnSnS_4 (CZTS) solar cells [1–3] is the increase of the open-circuit voltage (V_{OC}), i.e. the parameter that actually limits the devices efficiency [4–6]. A crucial aspect to obtain higher V_{OC} in CZTS is the optimization of the charge-extraction efficiency in the depletion region at the interface between CZTS and CdS. The alignment between the conduction bands of the CdS and the CZTS is "cliff" type [7, 8], with the CdS conduction band edge lower than that of CZTS. It is notorious that such alignment reduces the V_{OC} of the cell. A further limitation on the use of pure CdS in CZTS devices is related to its optical absorption. Indeed, CdS has an optical bandgap (Eg) of just 2.45 eV, which renders it non-transparent at wavelengths shorter than 500 nm. This spectral characteristic of CdS causes parasitic absorption with consequent reduction of the short circuit current density (J_{SC}) of CZTS cells [9]. Another critical aspect of the general use of cadmium is related to its toxicity towards humans and plants. As a consequence of its environmentally unfriendliness, the presence of cadmium in a device raises the problem of its disposal. Cadmium has been recognized as a critical raw material (CRM) [10] and its employment on large scale application should be then minimized, if not completely avoided. Among the possible alternative films of pure CdS, the solid solution of zinc and cadmium sulfides $Zn_xCd_{1-x}S$ or (Zn, Cd) S is one of the most promising: the introduction of an optimal molar ratio of zinc ($x = 0.35$ in the mixed sulfide corresponding to a bandgap of around 2.7 eV) in the buffer layer much improves the band alignment at the CZTS/$Zn_xCd_{1-x}S$ junction giving a V_{oc} increase of about 100 mV [11]. These interesting results were obtained depositing the mixed sulfide buffer layer by SILAR [11-13]. Chemical bath deposition (CBD) can represent a suitable method for

Electronic supplementary material The online version of this article (https://doi.org/10.1007/s10854-019-02796-7) contains supplementary material, which is available to authorized users.

✉ Mirko Congiu
mirko.congiu@uniroma1.it

1 Department of Chemistry, University of Rome, La Sapienza"00185 P.zzle Aldo Moro 5, Rome, Italy

2 Department of Chemistry, University of Turin, Via Giuseppe Verdi, 8, 10124 Turin, Italy

3 University of São Paulo State "UNESP", Av. Engenheiro Luiz Edmundo Carrijo Coube, 14-01, Bauru, SP, Brazil

4 ENEA Casaccia Research Center, via Anguillarese 301, 00123 Rome, Italy

the preparation of $Zn_xCd_{1-x}S$. Interesting results have been obtained so far in the literature using CDB to grow ZnS/CdS mixed buffers in CIGS solar cells [14]. With these premises, the first objective of our investigation is the comparison of CBD and precursor ink method as deposition techniques for $Zn_xCd_{1-x}S$ buffer. CBD is simpler and faster but, because of the lower solubility of the CdS (3.6×10^{-29}) compared to the ZnS (1.2×10^{-23}) [15], it could lead to the production of films with a non-homogeneous composition along the thickness. A higher cadmium content is to be expected in the layers deposited at the beginning of the process with formation of a Cd-rich buffer at the $Zn_xCd_{1-x}S$/CZTS interface. As a different strategy, the spraying of solution based on thiourea, cadmium and zinc acetates in methanol, is considered for the direct deposition of the buffer layer on the substrates. This kind of solution is commonly defined as “precursor ink” with reference to an ink in which the “pigment” is a mixture the chemical precursors of the desired material (*e.g.* a thin semiconducting film) [16, 17]. Once the precursor ink is sprayed and deposited onto the substrate, the resulting thin, dry film can be thermally converted into $Zn_xCd_{1-x}S$. Unlike CBD, the ink-jet technique does not involve the use of large volumes of solution. For this reason, different kinds of precursor inks are being studied and applied in the fabrication of large area solar cells devices such as perovskite and dye solar cells [18, 19]. Matter of fact, the use of large volumes of organic solvents as well as heavy metal solutions does not comply with the modern green-chemistry guidelines for future industrial applications, due to the large amount of wastes [20, 21]. When the equilibrium constant of the product of solubility (K_{PS}) in water is considered for ZnS ($K_{PS} = 1.2 \times 10^{-23}$ at room temperature, r.t.) and CdS ($K_{PS} = 3.6 \times 10^{-29}$ at r.t.) the difficulties inherent to the co-precipitation of the two compounds in the same reaction environment (as in the cases of both CBD and SILAR approaches) appear immediately evident being the precipitation of CdS thermodynamically much more favored than the one of ZnS. The different solubilities of ZnS and CdS prevent the formation of a mixed sulfide with a controllable stoichiometry since zinc will tend to be generally present at much lower concentrations in the resulting film of mixed sulfide. In this regard, the ink method bypasses such a drawback by exploiting a degradation process in which water is not involved. In fact, degradation occurs in a dry film in which solubility equilibria are not involved due to the lack of water on the reaction surface.

2 Experimental

The complete list of materials is provided in the supporting information (SI).

2.1 Chemical bath deposition (CBD)

Thin films of CdS and $Zn_xCd_{1-x}S$ were grown by CBD in aqueous solution on clean glass substrates using thiourea (TU) as sulfur source. $CdSO_4$ and $ZnSO_4$ were added to the chemical bath to obtain different Cd/Zn molar ratios i.e. 0.45, 0.67 and 1.33 (in the pristine solution). The temperature of the bath was maintained at 70 °C using a conventional laboratory hotplate. Sodium citrate (CIT) was used as complexing agent [22] to limit the activity of cadmium into the solution at the three concentration levels: 25; 37 and 50 mM. In all of the solutions, 17 mL of NH_4OH was added in order to obtain a solution with pH > 11 and induce the hydrolysis of TU. The processing time was also considered as variable for the control of the process and we considered the values of 15, 30, 45 and 60 min as processing time.

2.2 Precursor ink deposition

The precursor ink was obtained from stock solutions of 0.1 M cadmium acetate, $Cd(CH_3COO)_2$, and 0.1 M zinc acetate, Zn $(CH_3COO)_2$, in HPLC grade methanol (H_2O < 5%). In a volumetric flask, 3 mL of methanol was poured. Then 10 mg of TU were added in the flask. The solution was spiked with the desired amount of $Cd(CH_3COO)_2$ and Zn $(CH_3COO)_2$ using a micropipette. After spiking, the solution was made-up to 10 mL by further addition of methanol. This solution was stored in the dark at 5 °C for up to five days. Glass substrates (area: 2.5×2.5 cm^2) were carefully cleaned in the ultrasonic bath for 10 min with each of the three different solvents: deionized water, acetone and isopropanol. After cleaning, the substrates were dried under nitrogen flow and stored away from dust and moisture. The composition of $Zn_xCd_{1-x}S$ could be easily varied over the whole range $0 < x < 1$ by changing directly the ratio between the two initial solutions. The depositions were conducted in two steps: in the first step the substrate is covered drop-by-drop with the precursor ink (250 μl) and subsequently dried in vacuum to rapidly evaporate the solvent; in the second step the dry substrate is transferred into an oven with nitrogen atmosphere and kept at 250 °C for 30 min.

3 Spectrophotometric characterization

The transmittance (T) and reflectance (R) spectra of CZTS samples grown on soda-lime glass were recorded with a Perkin-Elmer LAMBDA 950 spectrophotometer equipped with a 150 mm integrating sphere. The absorption coefficient $\alpha(\lambda)$ was calculated employing the approximate equation:

$$\alpha(\lambda) = 1/d * \ln\left[(1 - R(\lambda))/T(\lambda)\right] \quad (1)$$

where d (in cm) is the thickness of the film, $R(\lambda)$ is its wavelength-dependent reflectance and $T(\lambda)$ is its wavelength-dependent transmittance. In this context, the reflectance measurement is compulsory in order to get a reliable estimation of $\alpha(\lambda)$, since reflectance variations are caused by both refractive index variation and interference effects (even for low thickness values). Since $Zn_xCd_{1-x}S$ is a semiconductor with direct bandgap, the value of the bandgap can be extracted from the "Tauc plot" [23], that is obtained by plotting $(\alpha h\nu)^2$ vs $h\nu$ (in eV), where α is the absorption coefficient of the film (in cm^{-1}).

4 GDOES characterization

The ratio between Cd and Zn into $Zn_{1-x}Cd_xS$ films was estimated through a depth profiling analysis of the samples performed by Glow Discharge Optical Emission Spectroscopy (GDOES) measurements using a Horiba Jobin Yvon GD Profiler 2 spectrometer with an anode diameter of 4 mm. The GDOES approach allows to analyze the chemical composition of a film throughout its thickness: indeed, a glow discharge sputters the film layer by layer and the removed atoms are then analyzed by their characteristic optical emission lines. Since the emission of Cd is stronger than that of Zn, it was necessary to normalize the two signals by comparing the spectrum of pristine sputtered ZnS with one of CdS deposited by CBD.

5 Results and discussion

5.1 CBD results

Experimentally, ZnCl and CdI were dissolved in the required concentration in deionized water containing cleaned glass slides. Then an aqueous solution of ammonium hydroxide (NH_4OH) was added to obtain a pH equal to 11 and heated up to 75 °C. An alkaline environment is required to allow the hydrolysis of thiourea, employed as S^{2-} source. The aqueous solution of thiourea, duly preheated, was added in the cation containing bath. After roughly 180 s, the bath solution starts yellowing as a proof of the initial nucleation of CdS or mixed $Zn_{1-x}Cd_xS$. The eventual formation of pure ZnS is hardly detectable, being the latter colorless. In order to investigate the effect of immersion time on the film properties, we removed the glass slides every 15 min up to one hour (Fig. 1a).

Chemical Bath Deposition (CBD) is a cheap and easy approach to obtain homogeneous films both at the surface and throughout the thickness of the layer. As reported in literature [11], the optimal Zn/Cd ratio in the film is 35/65. Yet, considering the different K_{ps} value of CdS (1×10^{-28}) and ZnS (3×10^{-25}) [24], the addition of a zinc salt in the bath is not enough to assure the formation of a mixed Sulfide.

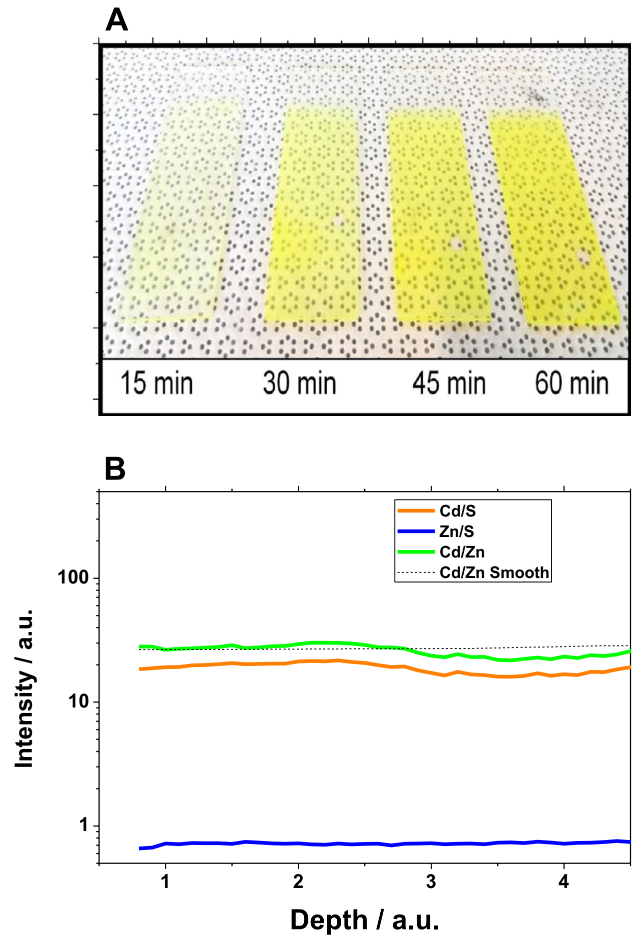

Fig. 1 **a** $Zn_{1-x}Cd_xS$ films obtained by CBD using a 9/1 Cd/Zn ratio and different deposition times. **b** Evaluation of the experimental Cd/Zn signal intensity ratio to calculate the multiplicative scaling factor to be used in $Zn_{1-x}Cd_xS$ samples. These measurements have been performed on pristine ZnS and CdS films

Indeed, the precipitation and the deposition of pure CdS is the thermodynamically favored path even though using a 100-fold more concentrated Zn-salt solution. Straightforwardly, an engineering of the deposition method is required.

The first characterizations performed on the films obtained through CBD were the determination of Eg through spectrophotometric measurements and Tauc's plot, and the estimation of Cd/S and Zn/S ratios on the films deposited varying the chemical bath composition through GDOES measurements. The experimental results are reported in Tables 1 and 2.

In order to compare the GDOES signals of Cd and Zn, one must consider that the strength of the emission signal depends on both the concentration and nature of the emitting element. For this reason, it was necessary to define a scaling factor to normalize the signals. This factor was calculated on pristine ZnS and CdS films. In both samples the signal of sulfur corresponds to an atomic concentration value close

Table 1 Comprehensive table of CBD experiments, each bath contains different concentrations of Zn, Cd and citrate (CIT)

Sample	CIT (mM)	[Zn^{2+}] (mM)	[Cd^{2+}] (mM)	[Cd/Zn][a]	[Cd/Zn][b] GDOES	Eg (eV)
ZnCdS_1	25	30	20	0.67	7	2.69
ZnCdS_2	50	15	20	1.33	22	2.62
ZnCdS_3	50	30	20	0.67	10	2.68
ZnCdS_4	25	45	20	0.45	4	2.7
ZnCdS_5	50	45	20	0.45	10	2.67
ZnCdS_6	37	45	20	0.45	6	2.69

[a]Cd/Zn in the chemical bath

[b]Cd/Zn in the films (GDOES)

Table 2 Linear regression coefficients considering Cd/Zn molar ratio and CIT concentration as independent variables and the observed Cd/Zn (GDOES) ratio in the final product as the dependent variable

Model	Coefficients[a]	
	B	SE
1		
(Constant)	− 7503	2087
Cd/Zn_ratio	14,695	1952
CIT	0.190	0.054

Dependent variable observed Cd/Zn (GDOES)

to 50%. The scale factor between Cd and Zn was therefore calculated as sputtering + ù between Cd/S and Zn/S in these two samples (Fig. 1) and its value was approximately 28. The Zn intensity in $Zn_xCd_{1-x}S$ samples was systematically multiplied by this factor to calculate the Zn/Cd ratio.

Another useful information from GDOES is the content of oxygen in the final product, in fact as the deposition occurs in strong alkaline conditions (pH > 11) there could exist a competition between the formation of metal oxide/hydroxide and sulfide. Considering two $Zn_xCd_{1-x}S$ samples, prepared using two different chemical baths with Cd/Zn concentration ratio of respectively 9/1 and 1/9, one can see that the bath richer in Zn produces films with a higher oxygen content (Fig. 2).

It is probably due to the formation of ZnO and $Zn(OH)_2$ on the substrates surface, leading to a mixed oxide/sulfide deposit. Notice that one of the advantage of metal sulfides over the corresponding oxides is the better electrical conductivity [25]. Moreover, the presence of mixed oxide/sulfide phase would heavily modify the electronic features of the films.

Sodium citrate (CIT) has been used as complexing agent for Cd^{2+} ions leading to a reduction of the concentration of the latter within the bath solution. Additionally, as we noticed during preliminary tests, the addition of CIT leads to more uniform films. The required amount of sodium citrate was added to the aqueous solution of cations before the addition of ammonium hydroxide. Three different [CIT] concentrations were tested, i.e. 25, 37.5 and 50 mM. By

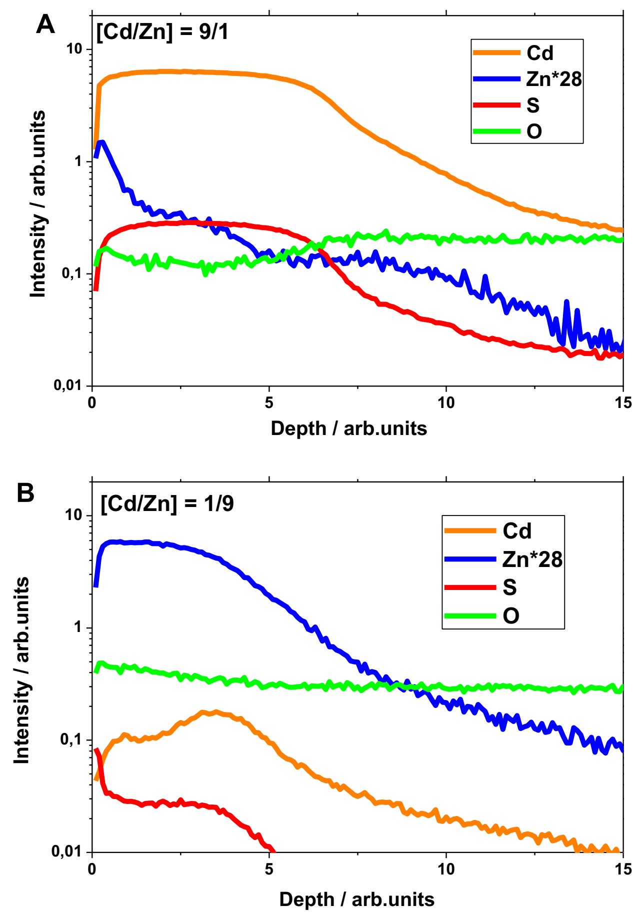

Fig. 2 GDOES profiles of two ZnCdS samples with nominal Cd/Zn ratios of 9/1 (**a**) and 1/9 (**b**). Notice that the chemical bath with the higher Zn concentration produces films in which the emission signal of oxygen is higher than that of sulfur

using a linear regression model, one can notice that both CIT and Cd/Zn molar ratio influence the final Cd/Zn ratio in the film estimated by GDOES.

The following equation (Eq. 2) represents the linear regression model used to estimate the effects of the solution composition over the final Cd/Zn ratio observed by GDOES.

$$Cd/Zn(GDOES) = B_1 * Cd/Zn + B_2 * CIT + k \quad (2)$$

where, B_1 and B_2 are the linear coefficients and k is a constant. The exhaustive results of the linear regression are provided in the SI. Our linear model well represents the experimental observations. In fact, the determination coefficient R^2 returned a value higher than 0.9. It means that more of the 90% of the variance of the independent variable is due to the variance in the assumed independent variable. The plot of the predicted Cd/Zn ratio versus the measured value is reported in Fig. 3.

From Fig. 3 one can notice that the distribution is closely linear ($R^2 = 0.965$). As expected, the value of the optical bandgap Eg is directly correlated to the effective Cd/Zn concentration in the solid solution $Zn_{1-x}Cd_xS$ (Fig. 4).

The values of Eg were calculated from Tauc's plot, by extrapolating the linear part of the plot of $(\alpha h\nu)^2$ vs $h\nu$ (Fig. 5b). The absorption coefficient α was calculated considering the films thickness.

The thickness of the film was measured by SEM cross-section images (Fig. 6) just for the samples deposited for 60 min (i.e. 100 nm, the thicker films of the samples set).

The thicknesses of the other samples (i.e. 15, 30 and 45 min) were calculated by scaling the absorption spectra of each with respect to the spectrum of the sample kept for 60 min (Fig. 5b). The scaling factor was used to estimate the thicknesses of all other samples assuming that the growth of the films is linear with time. From the data reported in Table 1 and the linear regression (Fig. 4) there is a clear correlation between the actual Cd/Zn ratio and the film bandgap, the lower the Cd/Zn ratio the higher the bandgap. The best result was obtained with a concentration of $CdSO_4$, $ZnSO_4$ and CIT of 20, 45 and 25 mM, respectively, a film

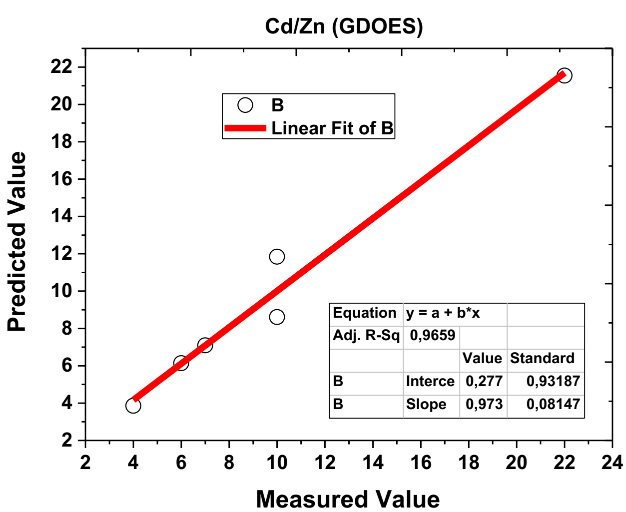

Fig. 3 Scatter plot of the predicted value (**b**) against the actual value (**a**) of Cd/Zn(GDOES) calculated using the linear regression model

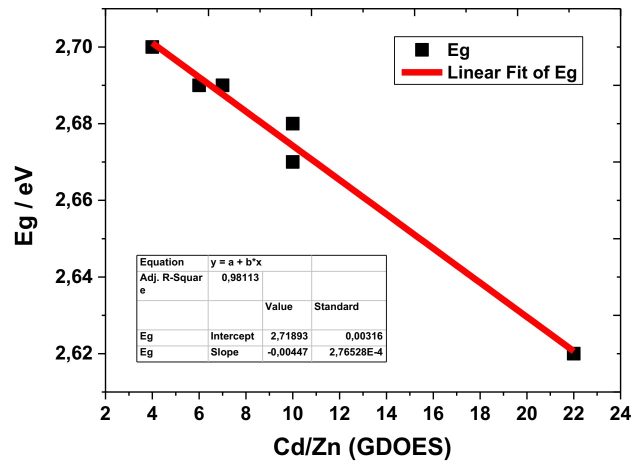

Fig. 4 Plot of the optical bandgap (Eg) against the measured Cd/Zn (GDOES). The linear fit of the data set shows a linear dependency of Eg from Cd/Zn ratio into the solid solution $Zn_{1-x}Cd_xS$ thin films.

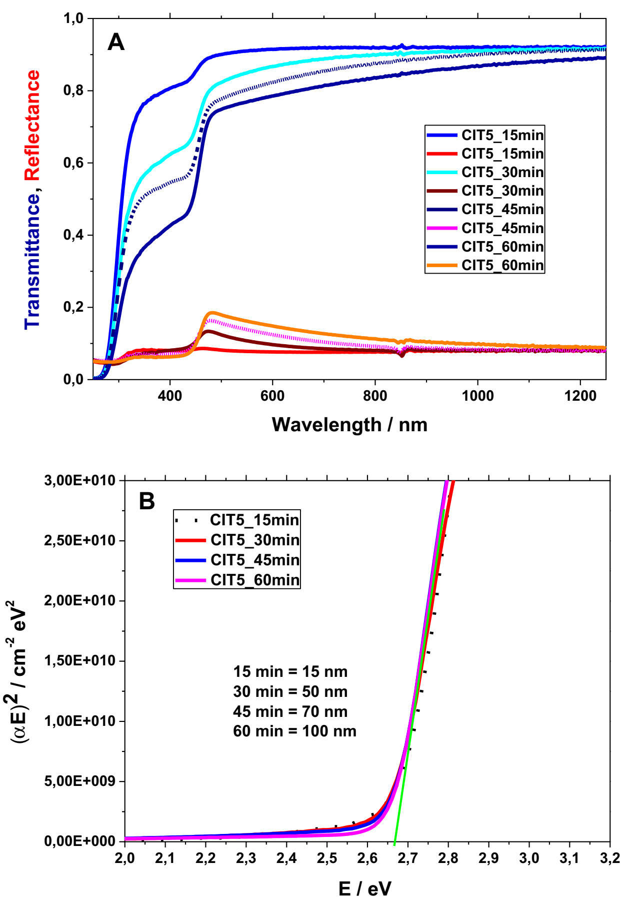

Fig. 5 **a** An example of transmittance measurements (blue) and reflectance (red) on the same set of samples with different deposition times. **b** Estimation of the thickness of the films obtained with different deposition times. The scaling factor was determined by mathematically equalize the linear parts of the plots (Color figure online)

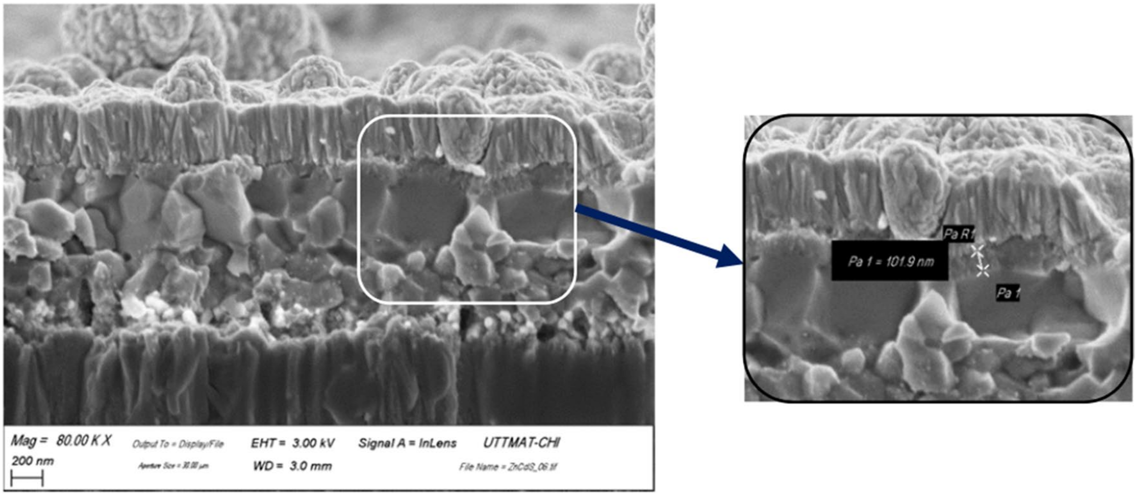

Fig. 6 SEM cross-section image of a typical CZTS device with $Zn_{1-x}Cd_xS$ buffer between the upper conducting layer (ITO) and the compact ZnO layer. The buffer was obtained through CBD for 60 min. The thickness of the buffer layer was directly measured on the cross-section

with bandgap higher than 2.7 eV corresponding to a nominal Cd/Zn ratio close to 4. The table also shows the large difference between the nominal composition of the films and the estimated by GDOES measurements: in all samples the actual concentration of zinc is lower than the nominal one probably due to the solubility equilibria of the different species in the solution. Another important parameter is the citrate concentration, the lower concentration of citrate the lower is the actual Cd/Zn ratio. Probably, when CIT is added to the solution there is a competition between the formation of Zn-CIT and Cd-CIT complexes. In fact, it is known that the stability constants of Cd-CIT complexes are higher than those of the corresponding Zinc complexes as reported by Capone et al. [26]. The effect of citrate is not substantially influenced by varying the concentrations of Cadmium and Zinc. It is worth mentioning that the strong alkaline environment (compulsory for the quantitative hydrolysis of thiourea) causes the formation of Zn and Cd hydroxides that are only partially soluble. Therefore, it must be considered that during the deposition of $Zn_{1-x}Cd_xS$, impurities of $Zn(OH)_2$ or $Cd(OH)_2$ can be incorporated. The K_{ps} of the two hydroxides are very similar (10^{-14} and 10^{-15} respectively) and in a strongly basic environment both tend to precipitate. In order to overcome the formation of hydroxides, the reduction of cations concentration as well as the acidification of the precursor solution are not feasible routes. Straightforwardly, we resolved by an innovative approach consisting in the acidification of the solution only after an initial yellowing (i.e. after the release of S^{2-} anions from thiourea). This leads to an evident slackening of the deposition reaction (thinner films). Some preliminary results highlighted a good homogeneity and interesting optical properties of the film. Yet, this method required a further engineering to finely control composition of the film and it will be investigated in detail in a forthcoming paper.

5.2 Results on films deposited through precursor ink

In these preliminary experiments, the ink-based method for the deposition of $Zn_{1-x}Cd_xS$ has been studied considering two nominal compositions ($x = 0.4$ and $x = 0.7$) as reported in Table 3. The first considered aspects were the volume of solution deposited per cm^2, the number of depositions, the heat treatment (temperatures and times) and above all the technique of drying the samples, crucial for obtaining homogeneous layers.

Figure 7 shows 3 samples of $Zn_{0.7}Cd_{0.3}S$_INK which, despite being nominally the same, have a different and non-homogeneous morphology due to different drying processes.

One of the main issues of the ink, at the actual state of the art, is the drying process. In fact, when the substrate is let too slowly dry at room temperature, we observed the formation of aggregates over the substrates surface. Through preliminary experiments, we concluded that the best drying process is to rapidly evaporate the solvent using a vacuum chamber to avoid the formation of aggregates. Vacuum evaporation leads to more uniform films even if some samples

Table 3 Comparison between the nominal and the actual values of Cd/Zn ratios observed in the samples prepared using two different inks

Sample	[Cd/Zn] nominale	[Cd/Zn] GDOES	Eg (eV)
$Zn_{0.7}Cd_{0.3}S$_INK	0.43	0.7	3.4–3.55

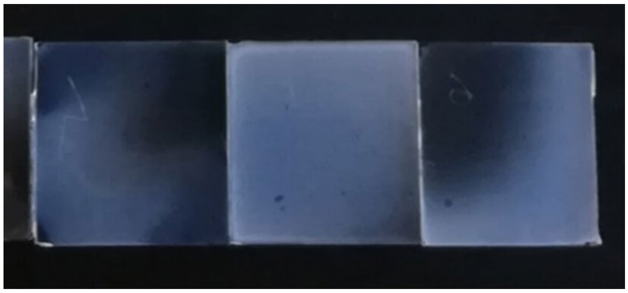

Fig. 7 A photograph of three glass slides samples (2×2 cm), covered with the precursor ink and vacuum-dried. The films present darker regions probably due the formation of a non-homogeneous film

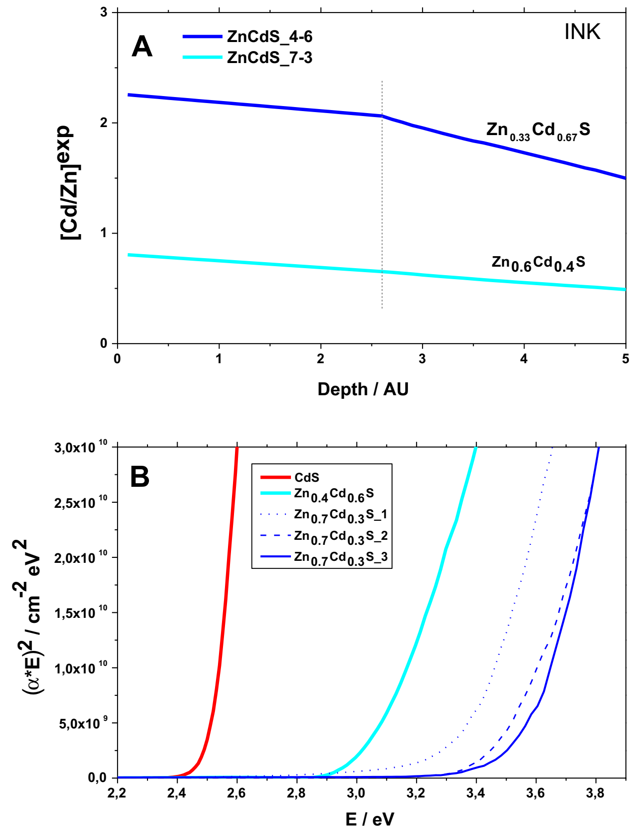

Fig. 8 Cd/Zn ratio obtained by GDOES in two different samples deposited on glass slides using different ink compositions (**a**). Tauc plots of pristine CdS, $Zn_{0.4}Cd_{0.6}S$ and three experimental replicates of $Zn_{0.7}Cd_{0.3}S$ samples. Notice that the differences in the optical bandgap is due to the inhomogeneity of the latter sample

of a same lot remain inhomogeneous (Fig. 7). Nevertheless, this aspect needs just for a technical optimization. One of the more affordable strategy is to try different solvents, or a mixture of them, to achieve an optimal composition, and this goal is beyond the aims of this paper. Just the samples with a homogeneous precursor layer were submitted to the thermal treatment to convert the precursors mixture to the respective sulfide solid solutions. The as mentioned experiments have shown that to obtain a good homogeneity it is necessary to dry the sample as quickly as possible by introducing it into a vacuum chamber followed by a faster and symmetrical pumping possible.

The samples obtained were characterized by spectrophotometric and GDOES measurements like the previous ones. These samples displayed energy gap values and Zn concentrations greater than the samples obtained by CBD, as shown in Fig. 8. In Table 3 one can see differences between the nominal value of the composition and that obtained through GDOES measurements, the later richer in cadmium. The samples deposited on glass substrates that showed the best composition and energy gap characteristics were deposited under the same conditions on CZTS to obtain functioning devices and thus characterize their opto-electronic properties. The preliminary results are provided within the supplementary information.

6 Conclusions

Two chemical deposition techniques have been reported to deposit $Zn_xCd_{1-x}S$ buffer layers for CZTS solar cells: Chemical Bath Deposition (CBD) and ink precursor technique (INK). In this study the influence of some experimental parameters on the film properties was analyzed in order to define the deposition conditions of buffer layers with appropriate composition and energy gap values. A linear regression model has been proposed to predict the final composition of the layer as a function of the experimental CBD conditions. The material bandgap was estimated from a Tauc plot of the absorption coefficient obtained by spectrophotometric measurements (T, R). Moreover, an innovative characterization technique based on GDOES measurements was developed to check the actual composition of the films. In the case of CBD there is a noticeable difference between the film and the bath composition, due to the fact that not all zinc present in the bath is incorporated in the film. The difference between measured and nominal composition is instead much smaller in the case of films obtained for INK.

CBD allowed to obtain $Zn_{1-x}Cd_xS$ films with good homogeneity and morphology in a reproducible way. There is still the need of optimizing the CBD procedure to further increase the gap value and improve the band alignment through the elimination of the contaminants zinc oxides and hydroxides. The ink deposition technique showed considerable operating advantages for a variety of reasons: speed of film preparation, width of the range of composition, use of small amounts of reagents (including the toxic ones that contain cadmium). The ink-based method must be further improved and optimized as far as the aspects of film morphology control and sample thickness are concerned. The replacement of thiourea with thioacetamide affords a higher homogeneity. These aspects related to the optimization of the various deposition methods here considered will be studied and presented in a forthcoming paper. It is suggested that different types of complexing agents need to be considered for the optimization of the chemical and opto-electronic characteristics of the mixed sulfide films.

7 Supporting information

Supporting Information is available from the Wiley Online Library or from the author.

Acknowledgements This work was supported by FAPESP (Grant Nno. 2016/17302-8) and from Sapienza, D.D. gratefully acknowledges the financial support from the project PAR 2016 (Progetto B.1.2 "Ricerca su tecnologie fotovoltaiche"/Accordo di Collaborazione ENEA–Dipartimento di Chimica dell' Università di Roma "La Sapienza").

References

1. H. Wang, Progress in thin film solar cells based on Cu_2 $ZnSnS_4$. Int. J. Photoenergy **2011**, Article ID 801292 (2011)
2. X. Song, X. Ji, M. Li, W. Lin, X. Luo, H. Zhang, A review on development prospect of CZTS based thin film solar cells. Int. J. Photoenergy **2014**, Article ID 613173 (2014)
3. M. Ravindiran, C. Praveenkumar, Status review and the future prospects of CZTS based solar cell—A novel approach on the device structure and material modeling for CZTS based photovoltaic device. Renew. Sustain. Energy Rev. **94**, 317–329 (2018)
4. A. Guchhait, Z. Su, Y.F. Tay, S. Shukla, W. Li, S.W. Leow, J.M.R. Tan, S. Lie, O. Gunawan, L.H. Wong, Enhancement of open-circuit voltage of solution-processed Cu_2ZnSnS_4 solar cells with 72% efficiency by incorporation of silver. ACS Energy Lett. **1**(6), 1256–1261 (2016)
5. M. Courel, J.A. Andrade-Arvizu, O. Vigil-Galán, Loss mechanisms influence on Cu_2ZnSnS_4/CdS-based thin film solar cell performance. Solid State Electron. **111**, 243–250 (2015)
6. A. Kumar, A.D. Thakur, Comprehensive loss modeling in Cu2ZnSnS4 solar cells. Curr. Appl. Phys. **19**(10), 1111–1119 (2019)
7. C. Yan, F. Liu, N. Song, B.K. Ng, J.A. Stride, A. Tadich, X. Hao, Band alignments of different buffer layers (CdS, Zn(O,S), and In 2S3) on Cu_2ZnSnS_4. Appl. Phys. Lett. **104**(17) (2014)
8. A. Crovetto, O. Hansen, What is the band alignment of $Cu_2ZnSn(S, Se)_4$ solar cells? Sol. Energy Mater. Sol. Cells **169**, 177–194 (2017)
9. M.B. Ortuño-López, M. Sotelo-Lerma, A. Mendoza-Galván, R. Ramírez-Bon, Optical bandgap tuning and study of strain in CdS thin films. Vacuum **76**(2–3), 181–184 (2004)
10. M. Hofmann, H. Hofmann, C. Hagelüken, A. Hool, Critical raw materials: a perspective from the materials science community. Sustain. Mater. Technol. **17**, e00074 (2018)
11. K. Sun, C. Yan, F. Liu, J. Huang, F. Zhou, J.A. Stride, M. Green, X. Hao, Over 9% efficient kesterite Cu_2ZnSnS_4 solar cell fabricated by using $Zn_{1-x}Cd_xS$ buffer layer. Adv. Energy Mater. **6**(12), 1600046 (2016)
12. M.A. Green, Y. Hishikawa, E.D. Dunlop, D.H. Levi, J. Hohl-Ebinger, A.W.Y. Ho-Baillie, Solar cell efficiency tables (version 52). Prog. Photovoltaics Res. Appl. **26**(7), 427–436 (2018)
13. M. Congiu, F. Decker, D. Dini, C.F.O. Graeff, An open-source equipment for thin film fabrication by electrodeposition, dip coating, and SILAR. Int. J. Adv. Manuf. Technol. (2016)
14. R.N. Bhattacharya, 195%-efficient $cuIn_{1-x}Ga_xSe_2$ photovoltaic cells using a Cd-Zn-S buffer layer. ECS Trans. **13**(17), 173–176 (2008)
15. M. Saidoun, K. Mateen, S. Baraka-Lokmane, and C. Hurtevent, Prediction of sulfide scales—improvement of our understanding of heavy metal sulfide solubility, in Soc. Pet. Eng. - SPE Int. Oilf. Scale Conf. Exhib. (2016)
16. I. Van Driessche, J. Feys, S.C. Hopkins, P. Lommens, X. Granados, B.A. Glowacki, S. Ricart, B. Holzapfel, M. Vilardell, A. Kirchner, M. Bäcker, Chemical solution deposition using ink-jet printing for YBCO coated conductors. Supercond. Sci. Technol. **25**(6), 065017 (2012)
17. S. Gamerith, A. Klug, H. Scheiber, U. Scherf, E. Moderegger, E.J.W. List, Direct ink-jet printing of Ag-Cu nanoparticle and Ag-precursor based electrodes for OFET applications. Adv. Funct. Mater. **17**(16), 3111–3118 (2007)
18. M. Yang, Z. Li, M.O. Reese, O.G. Reid, D.H. Kim, S. Siol, T.R. Klein, Y. Yan, J.J. Berry, M.F.A.M. Van Hest, K. Zhu, Perovskite ink with wide processing window for scalable high-efficiency solar cells. Nat. Energy **2**, 17038 (2017)
19. M. Congiu, A. Lanuti, A. di Carlo, C.F.O. Graeff, A novel and large area suitable water-based ink for the deposition of cobalt sulfide films for solar energy conversion with iodine-free electrolytes. Sol. Energy **122**, 87–96 (2015)
20. S.J. Ahn, S. Rehan, D.G. Moon, Y.J. Eo, S.K. Ahn, J.H. Yun, A. Cho, J. Gwak, An amorphous Cu-In-S nanoparticle-based precursor ink with improved atom economy for CuInSe2 solar cells with 1085% efficiency. Green Chem. **19**(5), 1268–1277 (2017)
21. K. Kim, I. Kim, Y. Oh, D. Lee, K. Woo, S. Jeong, J. Moon, Influence of precursor type on non-toxic hybrid inks for high-efficiency Cu2ZnSnS4thin-film solar cells. Green Chem. **16**(9), 4323–4332 (2014)
22. H. Yao, H. Shen, X. Zhu, J. Jiao, J. Li, W. Wang, Influence of Cd source concentration on photo-current response property of CdxZn1-xS film prepared by chemical bath deposition. Ceram Int **42**, 2466 (2016)
23. J. Tauc, Optical properties and electronic structure of amorphous Ge and Si. Mater. Res. Bull. **3**, 37 (1968)
24. M. Congiu, M.H. Boratto, C.F.O. Graeff, A synaptic electrochemical memristor based on the Cu^{2+}/Zn^{2+}cation exchange in Zn:CdS thin films. ChemistrySelect **3**(34), 9794–9802 (2018)
25. C. Vincent, B. Scrosati, *Modern Batteries*, 2nd edn. (Elsevier Science, Oxford, 1997)
26. S. Capone, A. De Robertis, C. De Stefano, S. Sammartano, Formation and stability of zinc(II) and cadmium(II) citrate complexes in aqueous solution at various temperatures. Talanta **33**(9), 763–767 (1986)